2009

Annealing effects on the optical properties of semiconducting boron carbide

R. B. Billa
University of Nebraska - Lincoln

Tino Hofmann
University of Nebraska - Lincoln, thofmann4@unl.edu

Mathias Schubert
University of Nebraska - Lincoln, mschubert4@unl.edu

Brian W. Robertson
University of Nebraska - Lincoln, brobertson1@unl.edu

Annealing effects on the optical properties of semiconducting boron carbide

R. B. Billa,[1,a)] T. Hofmann,[2] M. Schubert,[2] and B. W. Robertson[1]

[1]*Department of Mechanical Engineering and Nebraska Center for Materials and Nanoscience, University of Nebraska, Lincoln, Nebraska 68588, USA*
[2]*Department of Electrical Engineering and Nebraska Center for Materials and Nanoscience, University of Nebraska, Lincoln, Nebraska 68588, USA*

Infrared vibrations of as-deposited and annealed semiconducting boron carbide thin films were investigated by midinfrared spectroscopic ellipsometry. The strong boron-hydrogen resonance at ~ 2560 cm^{-1} in as-deposited films reveals considerable hydrogen incorporation during plasma-enhanced chemical vapor deposition. Extended annealing at 600 °C caused significant reduction in film thickness, substantial reduction of boron-hydrogen bond resonance absorption, and development of distinct blue-shifted boron-carbon and icosahedral vibration mode resonances. Our findings suggest that annealing results in substantial loss of hydrogen and in development of icosahedral structure, accompanied by strain relaxation and densification. © *2009 American Institute of Physics.* [DOI: 10.1063/1.3190679]

I. INTRODUCTION

In traditional form, boron carbide has a high melting point (2350 °C), outstanding hardness, and wear resistance. It is the third hardest material after diamond and cubic boron nitride.[1] A semiconducting form of boron carbide was proposed in 1959,[2] but only much more recently was the fabrication of boron carbide devices achieved, first using plasma-enhanced chemical vapor deposition (PECVD) of closo-1,2,-dicarbodecaborane (ortho-carborane, $C_2B_{10}H_{12}$).[3–5] Highly resistive boron carbide thin films have now been fabricated using a variety of CVD and physical vapor deposition techniques, including plasma decomposition of diborane and methane,[6,7] synchrotron radiation induced chemical vapor deposition,[8,9] and sputtering of boron carbide targets.[10,11] As a stable, nontoxic source of B and C, *ortho*-carborane has been successfully used to grow both *p*-type (self-doped) semiconducting boron carbide films on Si (Refs. 3–5) and SiC (Ref. 12) substrates, as well as *n*-type semiconducting boron carbide films (*ortho*-carborane doped with nickel-ocene, $Ni(C_5H_5)_2$) on Si.[13–16] PECVD boron carbide films, subsequently referred to as B_5C films, have been successfully used to make heterojunction diodes,[5,9,13,15] homojunction diodes,[15] tunnel diodes,[13,15] transistors,[5] magnetic tunnel junction devices,[17] and heteroisomeric diodes.[18,19]

Studies of structural influences on physical properties in semiconducting B_5C thin films are not exhaustive. The B_5C material is composed of light atoms with similar atomic numbers (boron, $Z=5$; carbon, $Z=6$; and possibly hydrogen, $Z=1$). Neither transmission electron microscopy (TEM) nor x-ray diffraction techniques clearly allow the atomic arrangements to be distinguished. Furthermore, TEM sample preparation by ion-milling techniques can alter the structure of semiconducting B_5C thin films.[20] Incorporation of hydrogen

in CVD-type semiconductor growth is common and affects the electrical and optical properties of many semiconductor materials.

In this work, we present an infrared spectroscopic ellipsometry (IRSE) study of the effect of annealing heat treatment on the structural properties of B_5C thin films. IRSE provides access to structural information of thin films, through measurement of their infrared dielectric function ε, and thereby to vibrational and free charge carrier excitation modes.[21] Characteristic vibrational frequencies were reported for boron carbide with compositions ranging from B_4C to $B_{10}C$ and with rhombohedral crystalline structure based on boron icosahedra.[22] The antisymmetric F_{1u}-symmetry breathing mode of two half-icosahedra occurs within the range of 1070–1090 cm^{-1}. The stretching vibration of the central B atom in the three-atom C–B–C chain at the center of the rhombohedral boron carbide structure occurs in the range of 1540–1580 cm^{-1}.[22] Saal *et al.*[23] predicted a substantial red-shift of this central chain vibration mode upon asymmetric C–B–C to B–B–C chain substitution. A characteristic B–H bond stretching mode was reported to occur around 2560 cm^{-1}.[6,24,25] Analysis of the B_5C thin film IRSE data presented here reveals strong variations of absorption resonances associated with boron-hydrogen and boron-carbon bond properties and development of an icosahedral signature accompanied by film thickness reduction on annealing.

II. THEORY AND EXPERIMENT

Previous optical studies of B_5C thin films employed spectrophotometry[3] in the near-infrared to ultraviolet spectral regions and spectroscopic ellipsometry (SE)[26] in the visible to ultraviolet regions and focused on band gap properties. SE determines the dielectric function ε and thickness d for thin films through best matching a parameterized model to measured data. The usual sample optical model for analyzing SE data is a sequence of parallel layers with perfectly abrupt

a)Electronic mail: ravi.billa@huskers.unl.edu.

interfaces and homogeneous ε, on a semi-infinite substrate.[27–29] Two approaches exist to determine ε for a thin film—point-by-point data inversion and model dielectric function (MDF) approximation. The point-by-point inversion often reveals subtle features which are otherwise subsumed by strong MDF line shape components.[28] The ellipsometric parameters Ψ and Δ are related to the complex-valued ratio ρ of the polarized plane wave components.[27] The equation

$$\rho = \frac{R_p}{R_s} = \tan(\Psi)e^{i\Delta}, \tag{1}$$

relates R_p and R_s, the complex-valued Fresnel reflection coefficients parallel (p), and perpendicular (s) to the plane of incidence. In addition to Ψ and Δ, standard deviations, σ_Ψ^{exp} and σ_Δ^{exp} are also estimated. The Levenberg–Marquardt[30] algorithm is used to fit the model parameters by minimizing a weighted test function[31] ξ^2,

$$\xi^2 = \frac{1}{2N-M}\sum_{j=1}^{N}\left[\left(\frac{\Psi_j^{mod}-\Psi_j^{exp}}{\sigma_{\Psi,j}^{exp}}\right)^2 + \left(\frac{\Delta_j^{mod}-\Delta_j^{exp}}{\sigma_{\Delta,j}^{exp}}\right)^2\right]. \tag{2}$$

Here, the number of measured $\Psi-\Delta$ pairs is N and the total number of real-valued fit parameters is M. The figure of merit (FOM) used to describe the confidence in the ith fit parameter is given by FOM=$1.65\sqrt{C_{ii}}\xi$. This is the usual one-parameter, 90%, uncorrelated confidence limit[30] multiplied by the test function ξ, where C_{ii} is the ith diagonal element of the fit parameter covariance matrix. In the case of a good fit with no systematic errors, ξ^2 tends toward a value of one and FOM$_i$ reduces to the standard 90% limit. The parameterized model comprises appropriate functions that best describe the line shapes in ε of the thin film. Here, Lorentzian-broadened harmonic oscillator functions proved sufficient to best match the experiment and calculated data for our B$_5$C thin film sample:

$$\varepsilon(\hbar\omega) = \varepsilon_{1\infty} + \sum_k \frac{A_k E_k B_k}{E_k^2 - (\hbar\omega)^2 - iB_k(\hbar\omega)}, \tag{3}$$

where A_k, E_k, and B_k represent the amplitude, center energy, and broadening of the kth oscillator, respectively, and $\varepsilon_{1\infty}$ is a good approximation of the squared index of refraction within the band gap.

B$_5$C thin film samples were prepared by PECVD of *closo*-1,2,- dicarbodecaborane (C$_2$B$_{10}$H$_{12}$; *ortho*-carborane)[3,4,9] on n-type (111) silicon substrates of resistivity of $10-100$ Ω cm, maintained at 350 °C during deposition. Annealing of samples was performed in a vacuum chamber with base pressure 1×10^{-6} Torr. The sample temperature was monitored and computer controlled by a thermocouple attached to the sample surface. Room temperature, normal ambient condition IRSE data were acquired from 600 to 3500 cm^{-1} with resolution of 4 cm^{-1} using a Fourier-transform based spectroscopic ellipsometer (IR-VASE™, J. A. Woollam Co.), at three angles of incidence (Φ_a =50°,60°,70°), before and after annealing at 600 °C for 24 h.
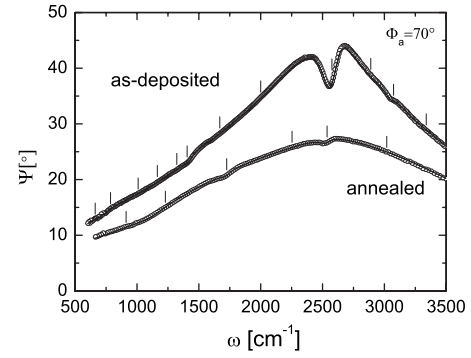

FIG. 1. Best-match calculated model (solid lines) and experimental (symbols) IRSE Ψ spectra from as-deposited B$_5$C thin film ($d=[656\pm1]$ nm) and after annealing at 600 °C for 24 h ($d=[502\pm1]$ nm). Vertical bars mark resonance frequencies of MDF oscillator contributions.

III. RESULTS AND DISCUSSION

Figure 1 depicts best-match model calculated and experimental IRSE Ψ data at Φ_a=70° before and after annealing, other Φ_a and Δ data being omitted for clarity. The MDF for best-match analysis of IRSE data obtained from as-deposited and annealed B$_5$C samples comprised different series of harmonic oscillators accounting for multiple infrared resonance absorption features. Table I summarizes the MDF parameters. Figure 2 depicts the point-by-point inverted and MDF imaginary parts of ε before and after annealing.

Both MDF and point-by-point inverted ε spectra match so closely that best-match calculated IRSE data are virtually indistinguishable from the experiment. The as-deposited and annealed sample ε spectra reveal multiple features, among which the strong features can be assigned to B–C and B–H

TABLE I. Best-match model calculated Lorentzian-broadened harmonic oscillator parameters for the as-deposited and annealed B$_5$C thin film samples.

| Assignment	E_k (cm^{-1})	A_k	B_k (cm^{-1})
	As-deposited B$_5$C ($\varepsilon_{1\infty}$=3.347$\pm$0.003)		
	662.0$\pm$2.3	0.815$\pm$0.004	368.7$\pm$5.9
	786.0$\pm$0.2	0.597$\pm$0.010	129.4$\pm$2.1
	1009.0$\pm$2.6	0.474$\pm$0.014	278.8$\pm$6.9
	1164.6$\pm$1.6	0.359$\pm$0.018	229.1$\pm$11.9
	1322.0$\pm$2.3	0.246$\pm$0.014	172.7$\pm$12.3
	1405.7$\pm$0.9	0.168$\pm$0.012	86.7$\pm$5.4
	1668.8$\pm$2.8	0.065$\pm$0.004	230.2$\pm$19.2
	2000.0$\pm$6.4	0.176$\pm$0.002	841.0$\pm$21.0
B–H	2576.8$\pm$0.3	0.297$\pm$0.001	115.6$\pm$1.2
	2890.0$\pm$6.9	0.027$\pm$0.002	247.1$\pm$31.6
	3074.8$\pm$3.0	0.027$\pm$0.002	84.6$\pm$13.3
	3338.0$\pm$13.5	0.073$\pm$0.001	894.2$\pm$42.1
	Annealed B$_5$C ($\varepsilon_{1\infty}$=4.706$\pm$0.004)		
	912.8$\pm$21.3	0.587$\pm$0.023	619.0$\pm$56.3
F_{1u}	1229.0$\pm$2.6	1.388$\pm$0.045	420.8$\pm$10.6
B–C	1725.6$\pm$1.6	0.128$\pm$0.005	90.0$\pm$6.5
	2253.6$\pm$8.4	0.064$\pm$0.007	580.9$\pm$63.8
B–H	2537.7$\pm$1.5	0.060$\pm$0.002	102.6$\pm$6.91
	3019.6$\pm$12.5	0.078$\pm$0.004	1227.4$\pm$69.8
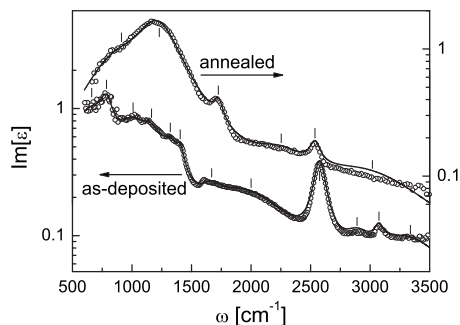
FIG. 2. Best-match point-by-point (symbols) and MDF (solid lines) derived $Im[\varepsilon]$ spectra for the B_5C thin film before and after annealing at 600 °C for 24 h. Vertical bars mark resonance frequencies of MDF oscillator contributions. Note the shifted ordinate (right) for the annealed case.

bond vibrations and to an F_{1u} antisymmetric icosahedral breathing mode.[22] For the as-deposited sample, a broad band occurs within the frequency ranges previously reported for rhombohedral boron and boron carbide,[22] and subtle resonances distributed within this region are consistent with an icosahedral nature of the B_5C thin film. Strong absorption is seen for the stretching mode B–H bond vibration, here at 2576 cm^{-1}, indicative of large incorporation of hydrogen.[6,24] On annealing, two distinct absorption features formed in icosahedral boron and B–C mode resonance regions, while the B–H mode has diminished considerably. The latter is indicative of hydrogen elimination during the annealing process. This change is accompanied by a 20% decrease in thin film thickness. Annealing clearly affected the density of the as-deposited B_5C thin films while forming well defined B–C bonds. Thus, it is evident that as-deposited B_5C thin films possess a low-order network of orthocarborane fragments, with large amounts of attached hydrogen. On annealing, the film structure changes, for example in its B–C bond lengths, as evidenced by the appearance of resonance features previously associated with rhombohedral boron and boron carbide structural arrangements. The characteristic B–C and icosahedral breathing mode resonances, however, occur strongly blue-shifted compared with rhombohedral crystalline boron and boron carbide.[22] This blue-shift points to a change in internal strain within the B_5C thin films on annealing. The relaxation of strain during annealing at elevated temperatures is well known and often observed in semiconductor heterostructures.[32] The strain-induced shift could be used as measure for the amount of strain, provided that appropriate deformation potential parameters are known, which they are not, yet, for B_5C thin films. The increase in density is also reflected in the increase in the $\varepsilon_{1\infty}$ parameter, which is directly proportional to the square of the index of refraction n within the band gap of B_5C thin films. The as-deposited parameter $\varepsilon_{1\infty}$ is in very good agreement with average n data within the visible to ultraviolet transparency region, obtained by SE investigations.[26] Here, the results lead to the conclusion that annealing increased the average band gap index of refraction value by ~18%.

IV. CONCLUSIONS

The optical properties of as-deposited and annealed semiconducting boron carbide thin films were investigated by midinfrared SE. MDF analysis identified a strong boron-hydrogen absorption feature at ~2560 cm^{-1} for the as-deposited B_5C thin films, indicative of hydrogen incorporation during deposition. Extended annealing at 600 °C caused the reduction of the B–H absorption feature and the formation of distinct B–C and icosahedral resonances. These reveal loss of hydrogen and structural thin film changes, accompanied by significant reduction in film thickness, densification and strain relaxation.

[1]K.-W. Lee and S. J. Harris, Diamond Relat. Mater. **7**, 1539 (1998).
[2]H. E. Robson, Ph.D. thesis, University of Kansas, 1959.
[3]S. Lee, J. Mazurowski, G. Ramseyer, and P. A. Dowben, J. Appl. Phys. **72**, 4925 (1992).
[4]S. Lee and P. A. Dowben, Appl. Phys. A: Mater. Sci. Process. **58**, 223 (1994).
[5]S.-D. Hwang, D. Byun, N. J. Ianno, and P. A. Dowben, Appl. Phys. Lett. **68**, 1495 (1996).
[6]S.-H. Lin, B. J. Feldman, and D. Li, Appl. Phys. Lett. **69**, 2373 (1996).
[7]J. Braddock-Wilking, S.-H. Lin, and B. J. Feldman, Tribol. Lett. **5**, 145 (1998).
[8]D. Byun, S.-D. Hwang, and P. A. Dowben, Appl. Phys. Lett. **64**, 1968 (1994).
[9]D. Byun, B. R. Spady, N. J. Ianno, and P. A. Dowben, Nanostruct. Mater. **5**, 465 (1995).
[10]A. F. Jankowski, L. R. Schrawyer, and M. A. Wall, J. Appl. Phys. **68**, 5162 (1990).
[11]A. F. Jankowski and P. L. Perry, Thin Solid Films **206**, 365 (1991).
[12]S. Adenwalla, P. Welsch, A. Harken, J. I. Brand, A. Sezer, and B. W. Robertson, Appl. Phys. Lett. **79**, 4357 (2001).
[13]S.-D. Hwang, N. B. Remmes, P. A. Dowben, and D. N. McIlroy, J. Vac. Sci. Technol. B **14**, 2957 (1996).
[14]S.-D. Hwang, N. Remmes, P. A. Dowben, and D. N. McIlroy, J. Vac. Sci. Technol. A **15**, 854 (1997).
[15]S.-D. Hwang, K. Yang, P. A. Dowben, A. A. Ahmad, N. J. Ianno, J. Z. Li, J. Y. Lin, H. X. Jiang, and D. N. McIlroy, Appl. Phys. Lett. **70**, 1028 (1997).
[16]D. N. McIlroy, S. D. Hwang, K. Yang, N. Remmes, P. A. Dowben, A. A. Ahmad, N. J. Ianno, J. Z. Li, J. Y. Lin, and H. X. Jiang, Appl. Phys. A: Mater. Sci. Process. **67**, 335 (1998).
[17]L. Bernard, J. Monson, A. Sokolov, Z.-Y. Liu, C. S. Yang, P. A. Dowben, B. Doudin, A. Harken, P. Welsch, and B. W. Robertson, Appl. Phys. Lett. **83**, 3743 (2003).
[18]A. N. Caruso, R. B. Billa, S. Balaz, J. I. Brand, and P. A. Dowben, J. Phys.: Condens. Matter **16**, L139 (2004).
[19]R. B. Billa, A. N. Caruso, and J. I. Brand, Mater. Res. Soc. Symp. Proc. **799**, 173 (2004).
[20]P. Lunca-Popa, J. I. Brand, S. Balaz, L. G. Rosa, N. M. Boag, M. Bai, B. W. Robertson, and P. A. Dowben, J. Phys. D **38**, 1248 (2005).
[21]M. Schubert, *Infrared Ellipsometry on Semiconductor Layer Structures* (Springer, New York, 2004).
[22]H. Werheit and H. Haupt, AIP Conf. Proc. **231**, 355 (1991).
[23]J. E. Saal, S. Shang, and Z.-K. Liu, Appl. Phys. Lett. **91**, 231915 (2007).
[24]S. C. Shen and M. Cardona, J. Phys. Colloq. **42**, 349 (1981).
[25]D. L. Schulz, A. Lutfurakhmanov, B. Mayo, J. Sandstrom, D. Bunzow, S. B. Qadri, R. Bao, D. B. Chrisey, and A. N. Caruso, J. Non-Cryst. Solids **354**, 2369 (2008).
[26]A. A. Ahmad, N. J. Ianno, P. G. Snyder, D. Welipitiya, D. Byun, and P. A. Dowben, J. Appl. Phys. **79**, 8643 (1996).
[27]R. M. A. Azzam and N. M. Bashara, *Ellipsometry and Polarized Light* (North-Holland, Amsterdam, 1977).
[28]M. Schubert, Ann. Phys. **15**, 480 (2006).

[29]C. M. Herzinger, P. G. Snyder, B. Johs, and J. A. Woollam, J. Appl. Phys. **77**, 1715 (1995).

[30]W. H. Press, S. A. Teukolsky, W. T. Vetterling, and B. P. Flannery, *Numerical Recipes: The Art of Scientific Computing* (Cambridge University Press, Cambridge, 2007).

[31]G. E. Jellison, Jr., Appl. Opt. **30**, 3354 (1991).

[32]H. J. Osten, J. Klatt, G. Lippert, B. Dietrich, and E. Bugiel, Phys. Rev. Lett. **69**, 450 (1992).